



HAL
open science

Effect of crosslinking by microbial transglutaminase of gelatin films on lysozyme kinetics of release in food simulants

Moslem Sabaghi, Catherine Joly, Isabelle Adt, Keziban Ozturk, Amandine Cottaz, Pascal Degraeve

► To cite this version:

Moslem Sabaghi, Catherine Joly, Isabelle Adt, Keziban Ozturk, Amandine Cottaz, et al.. Effect of crosslinking by microbial transglutaminase of gelatin films on lysozyme kinetics of release in food simulants. *Food Bioscience*, 2022, 48, pp.101816. 10.1016/j.fbio.2022.101816 . hal-04388584

HAL Id: hal-04388584

<https://univ-lyon1.hal.science/hal-04388584>

Submitted on 22 Jul 2024

HAL is a multi-disciplinary open access archive for the deposit and dissemination of scientific research documents, whether they are published or not. The documents may come from teaching and research institutions in France or abroad, or from public or private research centers.

L'archive ouverte pluridisciplinaire **HAL**, est destinée au dépôt et à la diffusion de documents scientifiques de niveau recherche, publiés ou non, émanant des établissements d'enseignement et de recherche français ou étrangers, des laboratoires publics ou privés.



Distributed under a Creative Commons Attribution - NonCommercial 4.0 International License

1 **Effect of crosslinking by microbial transglutaminase of gelatin films on lysozyme kinetics of**
2 **release in food simulants**

3

4 Moslem SABAGHI^{a,b}, Catherine JOLY^b, Isabelle ADT^b, Keziban OZTURK^b, Amandine
5 COTTAZ^b, Pascal DEGRAEVE^{b*}

6

7 ^aDepartment of Food Science and Technology, Gorgan University of Agricultural and Natural
8 Resources, Gorgan, Iran

9

10 ^bUniv Lyon, Université Claude Bernard Lyon 1, ISARA Lyon, BioDyMIA Research Unit,
11 Technopole Alimentec, 155 rue Henri de Boissieu, F-01000, Bourg en Bresse, France

12

13 E-mail address of each author

14

15 Moslem SABAGHI, Email address: m_sabaghi2@yahoo.co.uk

16 Catherine JOLY, Email address: catherine.joly@univ-lyon1.fr

17 Isabelle ADT, Email address: isabelle.adt@univ-lyon1.fr

18 Keziban OZTURK, Email address: keziban.ozturk@univ-lyon1.fr

19 Amandine COTTAZ, Email address: amandine.cottaz@univ-lyon1.fr

20

21 *Corresponding author's email: pascal.degraeve@univ-lyon1.fr

22 *Corresponding author's phone number: 00.33.(0)4.74.47.21.40

23

24 **Abstract**

25 The effect of enzymatic crosslinking by microbial transglutaminase on the physico-chemical
26 properties of gelatin-based films incorporated with lysozyme were investigated. Increase in the
27 crosslinking degree of gelatin with microbial transglutaminase concentration in film-forming
28 suspensions was correlated with a decrease of films thickness. Moreover, the enhancement in
29 crosslinking resulted in a decrease of the solubility in water, as well as of the extent of swelling
30 degree, and of the water vapor permeability of films and in an increase of films tensile strength.
31 The kinetics of release at 4°C of lysozyme from control non-reticulated films and reticulated
32 films to either sodium acetate buffer, or 2% (w/v) agar gels in direct contact were compared.
33 Interestingly, the kinetics of release of lysozyme were always slower from crosslinked films than
34 from control films. This difference was higher for lysozyme release to agar gels, which was
35 dominated by Fickian diffusion. Enzymatic crosslinking by microbial transglutaminase of
36 gelatin-based films incorporated with lysozyme can thus effectively control the release of this
37 food preservative.

38

39 **Keywords:** gelatin-based films, enzymatic crosslinking, microbial transglutaminase, lysozyme,
40 controlled release.

41

42 **List of abbreviations:**

43 ATR-FTIR spectroscopy: Attenuated Total Reflection - Fourier Transform InfraRed

44 spectroscopy

45 EAB: Elongation At Break

46 FFS: Film Forming Suspension

47 MTGase: Microbial TransGlutaminase

48 RH: Relative Humidity

49 RMSE: Root Mean Square Error

50 SSE: Sum of Squared estimate of Errors

51 TNBS: 2, 4, 6 TriNitroBenzene-1-Sulfonic acid

52 TS: Tensile Strength

53 WVP: Water Vapor Permeability

54 WVTR: Water Vapor Transmission Rate

55

56 **1. Introduction**

57 The shelf life of high-value refrigerated perishable foods (e. g., fish fillets, raw meat, cheese
58 slices...) is often limited by the growth of unwanted microorganisms on their surface (Odeyemi
59 et al., 2020). Therefore, different ways to deliver food preservatives in the superficial zone of
60 these foods, and thereby extend their shelf life have been proposed: (i) direct addition by
61 spraying a solution onto food surface, (ii) spraying, spreading, or dipping in a film-forming
62 suspension to get active coatings (Valdés et al., 2017), or (iii) addition in a film-forming
63 suspension, to get active stand-alone films that can be used to wrap perishable foods. Besides
64 providing a barrier to water molecules and oxygen uptake, the advantage of active coatings or
65 films over direct spraying of active molecules lies in their capacity to slow down their kinetics of
66 release. Controlled release of active molecules depends on the size of active molecules,
67 compared to the crosslinking density of networking of polymers forming the coating or the film,
68 on films porosity and tortuosity (Gemili et al., 2009), on the interactions between active
69 molecules and other coating/film constituents (mainly film-forming polymers), as well as on the
70 interactions between coating/film constituents and food constituents, namely water molecules.

71 Polysaccharides and proteins are biopolymers commonly used to prepare edible coatings or
72 films, due to their film-forming ability (Avramescu et al., 2020). However, one important
73 bottleneck to the broader use of coatings/films made with these edible biopolymers results from
74 their interactions with water, which is the main constituent of perishable foods. Indeed,
75 compared to conventional plastic films used for food packaging, all these materials have a far
76 lower water resistance (Castro-Rosas et al., 2016). Their higher water vapor permeability values
77 lead to accelerated drying of high moisture foods, and coating/film integrity loss can even result
78 from the dissolution of film-forming biopolymers by food moisture. A successful approach to

79 limit the dissolution of film-forming water-soluble biopolymers, such as gelatin, is their
80 crosslinking, which leads to an “irreversible” chemical network formed by covalently linked
81 macromolecules (Azeredo & Waldron, 2016). Microbial transglutaminase (MTGase) is applied
82 in food industries as an emulsifying, stabilizing, gelation, viscosifier, foaming, and water holding
83 agent. Ajinomoto company is the first commercial producer of MTGase since 1998. MTGase is
84 considered as GRAS (Generally Recognised As Safe) by Food and Drug Administration (FDA).
85 According to European Parliament Directive 2000/13 EC, MTGase is not an ingredient, but a
86 processing aid. Therefore, it is not listed in the ingredients of finished products (de Góes-Favoni
87 & Bueno, 2014). Enzymatic crosslinking of gelatin-based films by MTGase allowed thus to
88 reduce solubility in water of gelatin films from ~90% to ~60% (Kaewprachu et al., 2018; Ma et
89 al., 2020). Several authors reported the possibility to use such crosslinked gelatin-based films
90 incorporated with food preservatives, such as lysozyme or nisin, to extend the shelf life of
91 perishable foods (Kaewprachu et al., 2015, 2018). While it is known, in case of direct release of
92 bioactive agents from film matrix to food matrices, that excessive dissolution of polymers results
93 in less integrity of film matrix, and consequently in accelerated release of bioactive compound,
94 the effect of crosslinking by MTGase of gelatin-based films on the kinetics of release of
95 lysozyme has never been investigated. Therefore, in the present study, the kinetics of release of
96 lysozyme from control non-crosslinked gelatin-based films and from gelatin-based films
97 crosslinked by MTGase to aqueous buffer solutions or to an agarose gel mimicking the gel-like
98 structure of some perishable foods were compared. Besides its antimicrobial activity against
99 Gram-positive bacteria and its use as a food preservative, lysozyme is a 14.4 kDa globular
100 protein with a ~ 2 nm hydrodynamic radius: this higher molecular weight and size compared to
101 most food preservatives is expected to favor the decrease of its release kinetics from reticulated

102 films to the superficial zone of foods in direct contact. Moreover, lysozyme enzymatic activity
103 assay provides a specific and sensitive analytical method to monitor its release from films to
104 receptor media.

105

106 **2. Materials and Methods**

107

108 **2.1. Materials**

109 Bovine skin gelatin powder (gel strength ~ 225 g Bloom, type B) and hen egg white lysozyme
110 (70,000 units.mg⁻¹) were purchased from Sigma Aldrich (St Quentin Fallavier, France). MTGase
111 preparation (Activa TG-AK, Ajinomoto Foods Europe, Hamburg, Germany) contained 50-84
112 units.g⁻¹ corresponding to 0.6 g MTGase per 100 g, additional ingredients being anhydrous
113 trisodium phosphate (60 g per 100 g) and soy protein isolate, maltodextrins, and corn oil in
114 various proportions according to the manufacturer. Unless otherwise stated, all reagents were
115 from Sigma Aldrich.

116

117 **2.2. Gelatin films preparation**

118 Film-forming suspensions (FFS) contained 4.5 g.100 mL⁻¹ bovine gelatin, 0.9 g.100 mL⁻¹
119 glycerol as a plasticizer (i. e., 20% (w/w) of gelatin), 0.25 g.100 mL⁻¹ lysozyme, 0 (control),
120 0.14, 0.28, or 0.42 g.100 mL⁻¹ MTGase preparation. Gelatin stock suspension was prepared 24h
121 before use and stored at 4°C under continuous stirring **for a maximum of one day**. The pH of
122 gelatin stock suspension and lysozyme stock solution was adjusted to pH 5 by adding 0.01
123 mol.L⁻¹ HCl before FFS preparation. Each FFS was mixed at 45°C for 3h. Fifty milliliters of

124 each deaerated FFS were cast onto a 12cmx12cm Petri dish, and subsequently dried in an oven at
125 45°C for 24h. The final dried gelatin films were manually peeled.

126

127 **2.3. Determination of degree of crosslinking**

128 The degree of crosslinking of gelatin films was determined following the procedure described by
129 Prasertsung et. al (2010). Briefly, 5 mg of each film were weighed in a test tube and mixed with
130 1mL of 0.5% (w/v) 2, 4, 6 trinitrobenzene-1-sulfonic acid (TNBS) solution and 1mL of 4% (w/v)
131 sodium hydrogen carbonate buffer (pH=8.5). This mixture was then incubated for 2h at 40°C, so
132 that free amino groups of gelatin (not crosslinked) react with TNBS. Finally, 2 mL of 6 mol.L⁻¹
133 HCl were added to each tube before incubation for 90 min at 60°C. The absorbance at 415 nm of
134 each solution was then measured with a spectrophotometer after suitable dilution (Prasertsung et
135 al., 2010). The degree of crosslinking was calculated using equation (1):

$$136 \text{ Degree of crosslinking (\%)} = [1 - (\text{Abs}_{415\text{nm of crosslinked films}} / \text{Abs}_{415\text{nm of uncrosslinked films}})] \times 100 \quad (1)$$

137

138 **2.4. Physico-chemical properties**

139 To measure moisture content, solubility in water, and swelling index of films, 3.5 cm diameter
140 films were cut with a punch die and placed in a conditioning chamber (Vötsch Industrie Technik
141 GmbH, Balingen, Germany) for 48h at 23°C in a 50% relative humidity (RH) atmosphere.
142 Conditioned film weight (m_1) was measured. Moisture content was calculated according to
143 equation (2):

$$144 \text{ Moisture content (\%)} = ((m_1 - m_2) / m_1) \times 100 \quad (2)$$

145 where m_2 stands for the weight of films after 24 h drying at 75°C

146

147 Solubility in water of films at 20°C was calculated according to equation (3):

148 Solubility in water (%) = $((m_2 - m_3) / m_2) \times 100$ (3)

149 where m_3 stands for the dry weight (after 24h at 75°C) of films soaked a few seconds in double
150 distilled water before removing additional water (m_3) with a filter paper

151

152 Swelling index (%) of films was calculated according to equation (4):

153 Swelling index (%) = $((m_4 - m_1) / m_1) \times 100$ (4)

154 where m_4 stands for the weight of film after 24h conditioning at 23°C in a 50% RH atmosphere
155 following its soaking in double-distilled water and removal of additional water with a filter
156 paper.

157

158 **2.5. Water vapor transmission rate and permeability of films**

159 Water vapor transmission rates (WVTR) of gelatin films were determined at 23°C for a partial
160 pressure gradient equal to 33%-75% RH by the “wet cup” method (Cottaz et al., 2016). Briefly,
161 films preconditioned for 48h at 23°C in a 75% RH atmosphere were sealed on aluminum cups.
162 Grease was used to ensure water and air tightness at the contact zones. Aluminum cups were left
163 in a conditioning chamber at 23°C in an external atmosphere regulated at 75% RH and the
164 humidity of the internal atmosphere of cups was fixed at 33% RH with saturated $MgCl_2$ aqueous
165 solutions. The aluminum cups were periodically weighed to calculate the regression slope to
166 obtain the WVTR (equation 5) and the water vapor permeability (WVP) of films (equation 6).

167 $WVTR = \text{water uptake of cup (g)} / [\text{exposed area of film (m}^2\text{).time (days)}]$ (5)

168 $WVP = [\text{water uptake of cup (g)} \times (\text{film thickness (m)})] / [\text{exposed area of film (m}^2\text{). water vapor}$
169 $\text{pressure difference across film (Pa).time (s)}]$ (6)

170

171 **2.6. Mechanical properties**

172 Mechanical properties of films preconditioned at 23°C in a 50% RH atmosphere were
173 determined using a TA-HD-plus texture analyzer (Stable Micro Systems, Godalming, UK). The
174 films were cut into 6 cm x 1.5 cm rectangular strips. Grip separation was set at 40 mm. Samples
175 were clamped and deformed under tensile loading using a 1,000 N load cell with a crosshead
176 speed of 60 mm.min⁻¹ until samples were broken (Sabaghi et al., 2015). The maximum load and
177 the final extension at break were used for the calculation of tensile strength (TS) and elongation
178 at break (EAB), respectively.

179

180 **2.7. Evaluation of lysozyme release in buffer solution and agar gels**

181 Lysozyme release from crosslinked (0.42 g.100 mL⁻¹ MTGase) and non-crosslinked gelatin-
182 based films was first evaluated in 0.1 mol.L⁻¹ sodium acetate buffer (pH 7). Briefly, 0.5 cm
183 diameter films were immersed in 5 mL of sodium acetate buffer at 4°C to mimic refrigeration
184 temperature and left for 3 days in a rotary shaker (50 rpm) (IKA Loopster, Staufen, Germany).
185 These conditions accelerated release of lysozyme from films. Fifty microliters of buffer were
186 sampled out after 0, 1, 2, 4, 8 h, 1, 2 and 3 days and its lysozyme enzymatic activity was assayed
187 as described thereafter.

188 To mimic the release of lysozyme from gelatin films to semi-solid food matrices in direct
189 contact, crosslinked and non-crosslinked 3.5 cm diameter gelatin films with lysozyme were put
190 on the upper surface of 3.5 cm diameter and 5 mm height cylinders of 2% (w/v) agar gels for up
191 to 12 days at 4°C in a 75% RH atmosphere (0.05% (w/v) sodium azide was added in agar gels
192 formulation to prevent any microbial growth during these experiments). After 1 h, 2 h, 4 h, 8 h,

193 and every day from day 1 to day 12, agar cylinders were immediately cut into five 1 mm
194 thickness slices. Then, each agar gel slice was immediately immersed in 5 mL sodium acetate
195 buffer (0.1 mol.L⁻¹, pH 7) at 4°C for 24h under stirring conditions to extract lysozyme.

196 Lysozyme enzymatic activity of sodium acetate buffer solutions was assayed at 25°C with a
197 turbidimetric assay as described by Fabra et al. (2014). Lysozyme substrate was a *Micrococcus*
198 *lysodeikticus* cell suspension (0.16 g.L⁻¹) (M3770, Sigma Aldrich) in 0.1 mol.L⁻¹ sodium
199 phosphate buffer (pH 7). Fifty microliters of sodium phosphate buffer with released lysozyme
200 were added to 950 µL of *Micrococcus lysodeikticus* cell suspension. Turbidity was monitored for
201 2 min at 450 nm using a spectrophotometer (Uvikon, Northstar Scientific, Leeds, United
202 Kingdom). The initial slope of the 450 nm absorbance decrease as a function of time was used to
203 estimate the concentration of active lysozyme. One unit (U) of lysozyme activity was defined as
204 a 0.001 decrease in 450 nm absorbance in 1 min at 25°C (Bayarri et al., 2014). Lysozyme
205 activity assays were performed 3 times for each sample. The activity of released lysozyme was
206 calculated as the ratio between lysozyme activity assayed and the corresponding activity of the
207 quantity of lysozyme initially added in each film.

208 To investigate the kinetics of lysozyme release from gelatin films in food simulants, the
209 experimental data were fitted either with Higuchi (cumulative percentage of release versus
210 square root of time) (7), Ritger-Peppas (8), or Kopcha (9) equations.

211

212 $C = k.t^{0.5}$ (7)

213

214 $C = k.t^n$ (8)

215

216 $C = k_1 \cdot t^{0.5} + k_2 \cdot t$ (9)

217

218 where C stands for the concentration of released lysozyme at a given time (t), n is a release
219 coefficient. k is the Higuchi or Ritger-Peppas constant, respectively. k₁ and k₂ coefficients in
220 Kopcha equations are related to mass transport of lysozyme governed by Fickian diffusion or to
221 relaxation/diffusion of gelatin polymeric chains, respectively. A k₁ value higher than a k₂ value
222 indicates the predominance of Fickian diffusion in lysozyme transport.

223 Higuchi equation fits data corresponding to a release of active molecules driven by Fickian
224 diffusion. In the Ritger-Peppas equation, $n \leq 0.5$, indicates thus Fickian diffusion, while $0.5 < n < 1$
225 indicates non-Fickian transport (driven both by diffusion and erosion release behavior), and $n=1$
226 case-II transport (release in erosion mode).

227

228 **2.8. Attenuated total reflection - Fourier transform infrared (ATR-FTIR) spectroscopy**

229 Prior to ATR-FTIR analysis, samples, gelatin-based films with lysozyme before and after contact
230 with an agar gel (to simulate food contact with moist foods) were dried in a desiccator (silica gel,
231 RH= 0%) for 24h. ATR-FTIR spectra were then recorded using a diamond ATR crystal coupled
232 to an Alpha spectrometer (Bruker Optics , Wissembourg, France). Acquisition (accumulation of
233 32 scans) was performed in the wavenumber range from 500-3700 cm⁻¹ with a 2 cm⁻¹ resolution
234 (Cottaz et al., 2016).

235 Data were pre-processed using the OPUS (7.5 version) software from Bruker Optics (vectorial
236 normalization, smoothing (9 points) and rubber baseline correction) before peaks determination
237 (cut-off: 1%).

238

239 **2.9. Statistical analysis**

240 All experiments were performed in triplicate. All the data are provided as the mean values \pm SD
241 (standard deviation) (n=3). Two-way analysis of variance (ANOVA) by Fisher's test (F) was
242 used to compare the means. Difference was considered to be significant at $p < 0.05$. Fitting of
243 lysozyme release experimental data with the different models was performed with the help of
244 **Matlab™ version 7.10.0 (R2010a)** software (**The MathWorks Inc., Natick, MA**).

245

246 **3. Result and discussion**

247

248 **3.1. Effect of enzymatic crosslinking on the physico-chemical properties of gelatin-based** 249 **films**

250 Physico-chemical properties of films crosslinked by MTGase added at different concentrations in
251 the formulation of FFS and of control non-crosslinked films, which were conditioned at 23°C in
252 a 50% RH atmosphere before analysis, are presented in Table 1.

253 The addition of MTGase in the formulation of FFS resulted in a decrease in the number of free
254 amino groups reacting with TNBS in gelatin, as reflected by the increase of gelatin crosslinking
255 degree. Indeed, MTGase catalyzes the formation of isopeptide bonds between the γ -carboxamide
256 groups of glutamine residue side chains and the ϵ -amino groups ($-\text{NH}_2$) of lysine residue side
257 chains. While hen egg white lysozyme incorporated in film-forming suspensions contains 3
258 glutamine residues and 6 lysine residues in its 129-amino-acid sequence, native lysozyme, like
259 other globular proteins and unlike gelatin, is not a MTGase substrate (Murthy et al., 2009; Schuh
260 et al., 2010): the decrease in the number of free amino groups following MTGase action can thus
261 not be ascribed its action on lysozyme. Indeed, Kim and Uyama (2007) incubated 20% (w/v)

262 cold water fish gelatin for 24h at 37°C with 0.1-0.7 g.100 mL⁻¹ MTGase preparations: While
263 crosslinking degree significantly increased in the 0.1 to 0.4 g.100 mL⁻¹ MTGase preparation
264 range. Nevertheless, it did not significantly increase above this threshold MTGase concentration.
265 Present results with a limited increase of gelatin cross-linking degree when MTGase preparation
266 content in FFS increased from 0.28 to 0.42 g.100 mL⁻¹ are consistent with this 0.4 g.100 mL⁻¹
267 threshold concentration, above which no further increase of gelatin cross-linking degree was
268 observed. Kim and Umayya (2007) also reported that, for a fixed MTGase concentration,
269 crosslinking degree increased with gelatin concentration: this likely explains the high final
270 crosslinking degree of films (up to 52.1%±1.2%) after 24 h incubation at 45°C in an oven, since
271 these conditions result in water evaporation, and thus in a progressive increase of gelatin
272 concentration in films, thereby promoting enzymatic crosslinking of gelatin chains by MTGase.
273 As can be seen in Table 1, crosslinking by MTGase significantly decreased the thickness of the
274 gelatin films from 253±20 µm to 173±28 µm. Cheng et al. (2019) also applied MTGase as a
275 crosslinker to improve the structural properties of collagen films. These researchers concluded
276 that film thickness decreased due to the formation of a more compact structure.
277 However, crosslinking by MTGase (whatever its concentration in FFS) did not have any
278 significant (P > 0.05) effect on the moisture content of films pre-equilibrated at 23°C in a 50%
279 RH atmosphere. Indeed, Raja Mohd Hafidz et al. (2011) reported Lys (lysine) and Glx (glutamic
280 acid and glutamine) contents of bovine skin gelatin (11 and 34 residues per 1000 total amino acid
281 residues, respectively) were about twice lower than in porcine skin gelatin. Although the
282 formation of iso-peptide bonds between glutamine and lysine residues greatly affects other
283 gelatin properties, this did not significantly reduce the moisture content of films, likely due to the
284 limited decrease of hydrophilic groups along bovine skin gelatin chains resulting from the

285 formation of these bonds by MTGase. One must also consider, that films were not only plastified
286 by water, but also by glycerol, which represented 20% (w/w) of gelatin.

287 Among the physico-chemical properties of films, solubility in water at 20°C was the property
288 that was most affected by crosslinking by MTGase. Indeed, it decreased from 73.1%±4.7% for
289 control films to 27.3%±2.1% for films prepared with 0.14 g.100 mL⁻¹ MTGase preparation in
290 FFS. However, solubility in water at 20°C of crosslinked films did not further decrease for
291 higher MTGase concentrations in FFS. Consistently, the swelling index of films was
292 significantly lower for films crosslinked with MTGase (< 78.3%±1.3 %) compared to control
293 films (84.2%±4.9%). A similar decrease of the swelling index of chitosan-ovalbumin films and
294 of fish myofibrillar protein films crosslinked by MTGase was reported by Di Pierro et al. (2007)
295 and Kaewprachu et al. (2017). Cao et al. (2007) also observed a decrease of gelatin films
296 swelling index, when their crosslinking degree by either ferulic acid, or tannic acid increased. In
297 the present study, a decrease of swelling index likely results from crosslinking of gelatin chains,
298 inducing a less swollen films network. However, again, increasing MTGase preparation
299 concentration in FFS from 0.14 g.100 mL⁻¹ to 0.42 g.100 mL⁻¹ resulted in a limited decrease of
300 swelling index. This is consistent with the corresponding limited increase of crosslinking degree
301 and decrease of solubility in water.

302 Water vapor permeability (WVP) of gelatin films determined at 23°C for a partial pressure
303 gradient equal to 33%-75% RH (to simulate their use for the packaging of moist foods)
304 significantly decreased, when MTGase content of FFS increased: the WVP of films prepared
305 with 0.42 g.100 mL⁻¹ MTGase preparation in FFS was 33%±9% lower than that of control non-
306 crosslinked films. A similar decrease (23%±5%) was observed by Kaewprachu et al. (2018),

307 when comparing the WVP for a partial pressure gradient equal to 0%-100% RH at 30°C of
308 control gelatin films with nisin and catechin and that of the same films crosslinked by MTGase.
309 Crosslinking by MTGase of gelatin-based films with lysozyme resulted in a significant increase
310 of tensile strength of films. A similar increase was reported by Wu et al. (2017) for gelatin-based
311 films with natamycin also crosslinked by MTGase. An increase of tensile strength results from
312 the crosslinking of gelatin chains, thereby increasing the cohesiveness of the gelatin network.
313 Increasing MTGase concentration also resulted in an increase of elongation at break. The initial
314 increase of elongation at break with MTGase concentration in FFS also likely results from this
315 increase of cohesiveness of gelatin network in films. However, if crosslinking degree is too high,
316 this would increase film stiffness and thus decrease elongation at break. Bigi et al. (2001)
317 reported the increase of stiffness of gelatin-films reticulated by glutaraldehyde as a function of
318 the crosslinking degree of ϵ -amino groups along gelatin chains. In the present study,
319 intramolecular crosslinking acts as a chain extender, thus leading to a higher entanglement of
320 polymer chains.

321

322 **3.2. Effect of enzymatic crosslinking on the kinetics of release of lysozyme from gelatin-** 323 **based films**

324 The main goal of this study was to investigate how enzymatic crosslinking by MTGase of
325 gelatin-based films with lysozyme in their formulation can tune the kinetics of release of
326 lysozyme from these films to moist foods in direct contact. Therefore, the kinetics of release of
327 lysozyme from crosslinked and control gelatin-based films in sodium acetate buffer (0.1 mol.L⁻¹,
328 pH 7) were first compared (Figure 2A). Once immersed in buffer, each buffer-film combination
329 was placed in a rotary shaker to accelerate the kinetics of release of lysozyme from films.

330 Kinetics of release of lysozyme were monitored by assaying lysozyme activity in buffer at
331 regular intervals. After 4 h, more than 50% of lysozyme activity of control films was released,
332 unlike from crosslinked films. Indeed, the release of lysozyme from gelatin-based films to buffer
333 likely results both from partial solubilization of gelatin in buffer and from passive diffusion of
334 lysozyme in the gelatin network of films. Moreover, since films were in a rotary shaker, it can be
335 considered that lysozyme concentration in buffer was homogeneous, unlike when gelatin films
336 were placed in direct contact with agarose gel cylinders. At the beginning of desorption
337 experiments in stirred buffer, lysozyme concentration in buffer is close to zero: this results in a
338 higher lysozyme concentration gradient at the interface between films and surrounding medium
339 (buffer) and thus in accelerating lysozyme desorption compared to desorption under static
340 conditions.

341 Figure 2B shows the release rate of lysozyme from gelatin films in 2% (w/v) agar gel cylinders
342 in direct contact at 4°C for 288h (12 days). Agar gel was used as a simulant of semi-solid foods
343 and the temperature of 4°C mimicked refrigeration temperature. Following a progressive release
344 of lysozyme from control non-crosslinked films to agar gel in direct contact until 144h (day 6),
345 there was a sudden release of lysozyme from control films between 144h (day 6) and 168h (day
346 7): the release rate of lysozyme increased from 46.9% to 70.9%. This sudden release was likely
347 due to swelling of gelatin films, which favored mobility of gelatin chains and thus lysozyme
348 release. After 288h (12 days), 74.5% of total lysozyme was released from the control films.
349 Interestingly, the release rate of lysozyme from crosslinked films was lower and crosslinking of
350 films prolonged quasi-linear trend of lysozyme release kinetics up to 12 days. Nevertheless,
351 68.9% of total lysozyme was released from crosslinked films after 288 h (12 days). The effect of
352 enzymatic crosslinking of gelatin-based films on the depth of penetration of lysozyme in agar gel

353 in direct contact over time can also be observed in Figure 2B. Interestingly, while the quantity of
354 active lysozyme remained higher in the upper slice of agar gel, corresponding to a less than 1
355 mm depth of penetration, until 10 days of contact with control gelatin films, the quantity of
356 active lysozyme in this superficial zone of agar gel was higher than more in depth in the agar
357 cylinder during the 12 days of contact at 4°C with crosslinked films. This means that such
358 gelatin-based films with lysozyme crosslinked by MTGase can maintain a higher concentration
359 of lysozyme in this superficial zone for a longer time. Since most of contaminations by unwanted
360 microorganisms occur in this superficial zone of semi-solid high-moisture perishable foods, this
361 observation is promising for the rational design of active gelatin-based films with lysozyme to
362 extend the shelf life of such foods.

363 Such a possibility to slow down the kinetics of release of doxycycline from composite gelatin-
364 chitosan films (Tormos et al., 2015), of docetaxel drug model from conjugated casein hydrogel
365 (Yin et al., 2012), of lysozyme from sodium caseinate films (De Souza et al., 2010), or of
366 natamycin from gelatin films (Wu et al., 2017) by enzymatic crosslinking of these protein-based
367 films or hydrogels had already been reported in the literature. However, to our knowledge, this is
368 the first direct observation of the controlled release of lysozyme from gelatin-based films
369 crosslinked by MTGase. The slower release of lysozyme from crosslinked gelatin films might
370 result both from a decrease of the diffusion of lysozyme in the gelatin network of films, which is
371 likely denser and potentially less swollen as a result of enzymatic crosslinking of gelatin chains,
372 but also from a more limited solubilization of gelatin in the aqueous phase of agar gel.

373 Fitting the kinetics of release of lysozyme from films to either buffer or agar gel with different
374 controlled release models is a way to estimate the dominant mechanisms of transport of
375 lysozyme in these two experimental situations. Therefore, the fitting of experimental data with

376 Higuchi (cumulative percentage of release versus square root of time), Ritger-Peppas, or Kopcha
377 equations were compared (Table 2).

378 As judged by the R^2 values, Higuchi model could not fit the kinetics of release of lysozyme from
379 gelatin films to buffer. To find the best model with the highest correlation coefficient and the
380 lowest degree of freedom, the R^2 /RMSE coefficient was calculated. Ritger-Peppas and Kopcha
381 models with the highest R^2 /RMSE values (i. e. 15.11 and 6.93, respectively) were thus selected
382 as the best models for the release of lysozyme from control and from crosslinked gelatin films in
383 stirred buffer, respectively. Since a $n \leq 0.5$ value for Ritger-Peppas model was calculated for
384 control films (i. e. $n=0.17$), this indicates Fickian diffusion release behavior. For crosslinked
385 films, since k_1 value (0.28) exceeded k_2 value (0.02) calculated to fit the data with Kopcha
386 model, this also indicates that lysozyme kinetics of release from films to stirred buffer was
387 dominated by diffusion inside the films.

388 Regarding kinetics of release of lysozyme from control and crosslinked films to agar gels in
389 direct contact, Ritger-Peppas model was selected as the best model to fit the data with R^2 /RMSE
390 values of 9.52 and 11.77, respectively. Since calculated n values (0.37 and 0.4 for control and
391 crosslinked films, respectively) were both less than 0.5, this suggests that transport of lysozyme
392 from gelatin films to agar gels is mainly governed by Fickian diffusion.

393 Whatever the model, k or k_1 constants reported in Table 2 were always higher when modelling
394 release of lysozyme to stirred buffer, than when modelling its release to agar gels. This is
395 consistent with the fact that the first situation accelerates desorption of lysozyme from films.

396 Indeed, when comparing modelling of kinetics of release of lysozyme in buffer under constant
397 stirring conditions and in agar gels in direct contact, one must keep in mind, that, in the former
398 case, kinetics of desorption of lysozyme from films to the surrounding buffer are the limiting

399 factor, while, in the second case, desorption of lysozyme from films to the surface of gels results
400 in its accumulation at the vicinity of films: this results in the increase of lysozyme concentration
401 in the zone of gel in direct contact and thus in a decrease of the gradient of concentration of
402 lysozyme between films and their surface, which slows down its release kinetics.

403

404 **3.1. Fourier-transform infrared (FTIR) spectroscopic analysis of films**

405 FTIR spectroscopic analysis results are presented in Figure 3 (wavenumbers 3700-2700 cm^{-1} (A)
406 and 1800-800 cm^{-1} (B)) and in Table 3 (attribution of characteristic bands of films spectra). Five
407 typical zones have been identified in FTIR spectra of films. In wavenumber 2950-2850 cm^{-1}
408 region (Fig. 3A), two bands, which can be attributed to asymmetric (around 2940 cm^{-1}) and
409 symmetric (2875 cm^{-1}) vibrations of CH or CH_2 (Nandiyanto et al., 2019), were observed. The
410 contribution of this region is minor, which was expected, considering that these groups are
411 poorly represented in proteins like gelatin, in contrast with lipids.

412 Four domains specific of proteins are present:

413 - amide A and B (around 3270-3290 cm^{-1}), major region

414 - amide I (around 1620-1650 cm^{-1}), major region

415 - amide II (around 1520-1535 cm^{-1}), major region

416 - amide III (around 1237 cm^{-1}).

417 Moreover, lower wavenumbers can be attributed to short peptides chains (1080 cm^{-1}) and/or to
418 interactions between glycerol and gelatin ($\approx 1030 \text{ cm}^{-1}$) (Table 3).

419 Like in previous studies (Nagarajan et al., 2012; Wang et al. 2015; Liu et al., 2017), changes in
420 gelatin FTIR spectra were observed following enzymatic crosslinking of gelatin-based films by
421 MTGase. These modifications concern mainly the three major amide regions (amides A and B

422 region and amides I and II regions), suggesting changes in the secondary structure and in
423 functional groups. Addition of lysozyme in crosslinked films formulation induced some new
424 conformational changes in FTIR spectrum of gelatin in the same zones. Nevertheless, some of
425 these modifications were still observed after lysozyme release (Figure 3), likely because not all
426 lysozyme was released from films: indeed, only 68.9% of lysozyme activity initially loaded in
427 crosslinked gelatin films was recovered after 12 days contact with agarose gels.

428 Amide A band wavenumber was similar in control and crosslinked films without lysozyme,
429 while a clear shift from 3077 to 3070 cm^{-1} of amide B band was observed following gelatin
430 crosslinking by MTGase. According to Barth (2007), hydrogen bonds stabilize the structure of
431 proteins, and FTIR spectroscopy can be used to determine the strength of hydrogen bonds. More
432 precisely, as a general rule, hydrogen bonding lowers the frequency of stretching vibrations,
433 since it lowers the restoring force, but increases the frequency of bending vibrations, since it
434 produces an additional restoring force. Considering that the mechanism of activity of MTGase
435 consists in building isopeptide bonds between Gln and Lys residues of gelatin, a decrease of IR
436 wavenumbers of amide B and amide A bands was expected, but with higher differences notably
437 for amide A band. The lack of effect of enzymatic crosslinking on FTIR spectra of gelatin-based
438 films could be notably explained by the gelatin preparation process. Thus, normally a free NH
439 stretching associated to amide A band exhibits a frequency a 3400-3440 cm^{-1} but, gelatin
440 preparation procedures which are using heating at high temperature (100°C) lead to lower the
441 wavenumbers at around 3280 cm^{-1} (Nagarajan et al., 2012). This could explain that the amide A
442 couldn't be used as a crosslinking indicator in our studies (notably if the crosslinking degree is
443 low). However, Nagarajan and collaborators also mentioned that lowest amide B wavenumber
444 suggests the interactions of NH_3 group between peptide chains [30].

445 The incorporation of lysozyme induced a slight decrease of amide A bands and in contrast an
446 increase of amide B one. After lysozyme release, the 2 bands are shifting, these observations
447 suggest that lysozyme could have modified the stability of gelatin network.

448 In amide I region, Wang et al (2015) observed a band shift from 1641 to 1637 cm^{-1} . Crosslinking
449 with transglutaminase highest concentration (8U/g) induced a highest band shift. These
450 researchers concluded that increasing the concentration of MTGase favoured conformational
451 changes of the secondary structure of proteins. In the present study, a slight shift from 1629 to
452 1627 cm^{-1} was observed, while no differences were observed in amide II region.

453 To describe changes in amide III region, Wang et al (2015) observed that the crosslinking of
454 gelatin network by MTGase leads to an increase of amide I bands and a decrease of amide III
455 bands. This effect is enhanced when increasing MTGase concentration. Consistently with these
456 observations, an increase of amide I band intensity was also observed in our study. However, non
457 significant effect on amide III band was observed. Furthermore, we also noted a decrease of
458 amide B band. The 2 bands around 1030 and 1080 cm^{-1} can notably be attributed to C-O
459 stretching vibrations of short peptides chains and to the interactions between glycerol and gelatin
460 (Nagarajan et al., 2012). Interestingly, the 1080/1030 cm^{-1} ratio was positive for crosslinked
461 films without lysozyme and crosslinked films after lysozyme release, while it was negative for
462 the two other analysed films (control gelatin film and crosslinked film with lysozyme).

463

464 **4. Conclusion**

465

466 Enzymatic crosslinking of gelatin-based films by MTGase resulted in a decrease of their
467 solubility in water from $73.1\% \pm 4.7\%$ to $25.3\% \pm 2.3\%$. Interestingly, besides improving other

468 physical properties of films such as their tensile strength, enzymatic crosslinking of gelatin-based
469 films incorporated with lysozyme significantly decreased the kinetics of release of this food
470 preservative to food simulants (buffer or agar gel placed in direct contact). Enzymatic
471 crosslinking of gelatin-based films containing lysozyme is thus promising to design edible films
472 extending the shelf life of some perishable foods by inhibiting the growth of lysozyme-sensitive
473 bacteria.

474

475 **Declaration of competing interest:** The authors confirm that they have no conflicts of interest
476 with respect to the work described in this manuscript.

477

478 **Acknowledgements**

479 Ministry of Science, Research and Technology (Iran) is acknowledged for supporting the stay of
480 Dr Moslem SABAGHI (University of Gorgan) in BioDyMIA research unit. “Bourg en Bresse
481 Agglomération” and “Conseil Départemental de l’Ain” are acknowledged for financial support
482 of BioDyMIA research unit activities. The authors would like to thank Ajinomoto Co. Inc.
483 (Kawasaki, Japan) for Activa-TG-AK MTGase preparation gift.

484 **5. References**

485 Avramescu, S.M., Butean, C., Popa, C.V., Ortan, A., Moraru, I., & Temocico, G. (2020). Edible
486 and functionalized films/coatings - Performances and perspectives. *Coatings*, 10(7), 687.
487 Azeredo, H.M. & Waldron, K.W. (2016). Crosslinking in polysaccharide and protein films and
488 coatings for food contact - A review. *Trends Food Sci. Technol.*, 52, 109-122.
489 Barth, A. (2007). Infrared spectroscopy of proteins. *Biochim. Biophys. Acta - Bioenerg.*, 1767(9),
490 1073-1101.

491 Bayarri, M., Oulahal, N., Degraeve, P., & Gharsallaoui, A. (2014). Properties of lysozyme/low
492 methoxyl (LM) pectin complexes for antimicrobial edible food packaging. *J. Food Eng.*,
493 131, 18-25.

494 Bigi, A., Cojazzi, G., Panzavolta, S., Rubini K., & Roveri, N. (2001). Mechanical and thermal
495 properties of gelatin films at different degrees of glutaraldehyde crosslinking. *Biomater.*,
496 22(8), 763-768.

497 Cao, N., Fu, Y., & He, J. (2007). Preparation and physical properties of soy protein isolate and
498 gelatin composite films. *Food Hydrocoll.*, 21(7), 1153-1162.

499 Castro-Rosas, J., Cruz-Galvez, A.M., Gomez-Aldapa, C.A., Falfan-Cortes, R.N. Guzman-Ortiz,
500 F.A., & Rodríguez-Marín, M.L. (2016). Biopolymer films and the effects of added lipids,
501 nanoparticles and antimicrobials on their mechanical and barrier properties: a review. *Int.*
502 *J. Food Sci. Technol.*, 51(9), 1967-1978.

503 Cheng, S., Wang, W., Li, Y., Gao, G., Zhang, K., Zhou, J., & Wu, Z. (2019). Cross-linking and
504 film-forming properties of transglutaminase-modified collagen fibers tailored by
505 denaturation temperature. *Food Chem.*, 271, 527-535.

506 Cottaz, A., Khalil, F., Galland, S., Jbilou, F., Adt, I., Degraeve, P., & Joly, C. (2016).
507 Poly(butylene succinate-co-butylene adipate)/polyethylene oxide blends for controlled
508 release materials: A morphological study. *J. Appl. Polym. Sci.*, 133(3), 42874.

509 De Góes-Favoni, S.P. & Bueno, F.R. (2014). Microbial transglutaminase: general characteristics
510 and performance in food processing technology. *Food Biotechnol.*, 28(1), 1-24.

511 De Souza, P.M., Fernández, A., López-Carballo, G., Gavara, R., & Hernández-Muñoz, P. (2010).
512 Modified sodium caseinate films as releasing carriers of lysozyme, *Food Hydrocoll.*,
513 24(4), 300-306.

514 Di Pierro, P., Chico, B., Villalonga, R., Mariniello, L., Masi, P., & Porta, R. (2007).
515 Transglutaminase-catalyzed preparation of chitosan–ovalbumin films. *Enz. Microb.*
516 *Technol.*, 40(3), 437-441.

517 Fabra, M.J., Sánchez-González, L., & Chiralt, A. (2014). Lysozyme release from isolate pea
518 protein and starch based films and their antimicrobial properties. *LWT - Food Sci.*
519 *Technol.*, 55(1), 22-26.

520 Gemili, S., Yemenicioğlu, A., & Altinkaya, S.A. (2009). Development of cellulose acetate based
521 antimicrobial food packaging materials for controlled release of lysozyme. *J. Food Eng.*
522 *90(4)*, 453-462.

523 Hafidz, R., Yaakob, C., Amin, I., & Noorfaizan, A. (2011). Chemical and functional properties
524 of bovine and porcine skin gelatin. *Int. Food Res. J.*, 18(2), 813-817.

525 Kaewprachu, P., Osako, K., Benjakul, S., & Rawdkuen, S. (2015). Quality attributes of minced
526 pork wrapped with catechin-lysozyme incorporated gelatin film. *Food Packag. Shelf Life*,
527 *3*, 88-96.

528 Kaewprachu, P., Osako, K., Benjakul, S., Suthiluk, P., & Rawdkuen, S. (2017). Shelf life
529 extension for Bluefin tuna slices (*Thunnus thynnus*) wrapped with myofibrillar protein
530 film incorporated with catechin-Kradon extract. *Food Control*, 79, 333-343.

531 Kaewprachu, P., Ben Amara, C., Oulahal, N., Gharsallaoui, A., Joly, C., Tongdeesoontorn, W.,
532 Rawdkuen, S. & Degraeve, P. (2018). Gelatin films with nisin and catechin for minced
533 pork preservation. *Food Packag. Shelf Life*, 18, 173-183.

534 Kim, Y.-J. & Uyama, H. (2007). Biocompatible hydrogel formation of gelatin from cold water
535 fish via enzymatic networking. *Polym. J.*, 39(10), 1040-1046.

536 Liu, F., Chiou, B.-S., Avena-Bustillos, R.J., Zhang, Y., Li, Y., McHugh, T.H., & Zhong, F.
537 (2017). Study of combined effects of glycerol and transglutaminase on properties of
538 gelatin films. *Food Hydrocoll.*, 65, 1-9.

539 Ma, Y., Yang, R., & Zhao, W. (2020). Innovative water-insoluble edible film based on
540 biocatalytic crosslink of gelatin rich in glutamine. *Foods*, 9(4), 503.

541 Murthy S.N.P., Lukas T.J., Jardetzky T.S., & Lorand, L. (2009). Selectivity in the post-
542 translational transglutaminase-dependent acylation of lysine residues. *Biochem.*, 48,
543 2654-2660.

544 Nagarajan, M., Benjakul, S., Prodpran, T., Songtipya, P., & Kishimura, H. (2012).
545 Characteristics and functional properties of gelatin from splendid squid (*Loligo*
546 *formosana*) skin as affected by extraction temperatures. *Food Hydrocoll.*, 29(2), 389-397.

547 Nandiyanto, A.B.D., Oktiani, R., & Ragadhita, R. (2019). How to read and interpret FTIR
548 spectroscopy of organic material. *Indones J. Sci. Technol.*, 4(1), 97-118.

549 Odeyemi, O.A., Alegbeleye, O.O., Strateva, M., & Stratev D. (2020). Understanding spoilage
550 microbial community and spoilage mechanisms in foods of animal origin. *Compr. Rev.*
551 *Food Sci. Food Saf.*, 19(2), 311-331.

552 Prasertsung, I., Mongkolnavin, R., Kanokpanont, S., & Damrongsakkul, S. (2010). The effects of
553 pulsed inductively coupled plasma (PICP) on physical properties and biocompatibility of
554 crosslinked gelatin films. *Int. J. Biol. Macromol.*, 46(1), 72-78.

555 Romeih, E., & Walker, G. (2017). Recent advances on microbial transglutaminase and dairy
556 application. *Trends Food Sci. Technol.*, 62, 133-140.

557 Sabaghi M., Maghsoudlou Y., & Habibi P. (2015). Enhancing structural properties and
558 antioxidant activity of kefir films by chitosan addition. *Food Struct.*, 5, 66-71.

559 Schuh S., Schwarzenbolz U., & Henle T. (2010). Cross-linking of hen egg white lysozyme by
560 microbial transglutaminase under high hydrostatic pressure: localization of reactive
561 amino acid side chains. *J. Agric. Food Chem.*, 58, 12749-12752.

562 Tormos, C.J., Abraham, C., & Madihally, S.V. (2015). Improving the stability of chitosan-
563 gelatin-based hydrogels for cell delivery using transglutaminase and controlled release of
564 doxycycline. *Drug Deliv. Transl. Res.*, 5(6), 575-584.

565 Valdés, A., Ramos, M., Beltrán, A., Jiménez, A., & Garrigós, M.C. (2017). State of the art of
566 antimicrobial edible coatings for food packaging applications. *Coatings*, 7(4), 56.

567 Wang, Y., Liu, A., Ye, R., Wang, W., & Li, X. (2015). Transglutaminase-induced crosslinking
568 of gelatin-calcium carbonate composite films. *Food Chem.*, 166, 414-422.

569 Wu, X., Wang, K., Liu, Y., Liu, A., & Ye, R. (2017). Microstructure of transglutaminase-
570 induced gelatin-natamycin fungistatic composite films. *Int. J. Food Prop.*, 20(12), 3191-
571 3203.

572 Yin, W., Su, R., Qi W., & He, Z. (2012). A casein-polysaccharide hybrid hydrogel cross-linked
573 by transglutaminase for drug delivery. *J. Mater. Sci.*, 47(4), 2045-2055.

574

575 **Figure captions**

576 **Figure 1:** Schematic representation of experiments to monitor kinetics of release of lysozyme from
577 gelatin-based films to 2% (w/v) agar gels.

578 **Figure 2:** (A) Kinetics of release of lysozyme from crosslinked (red circle) and non-crosslinked (blue
579 triangle) gelatin-based films in the buffer. (B) Kinetics of release of lysozyme from crosslinked
580 (unfilled column) and non-crosslinked (filled column) gelatin-based films to 5 mm height agar gel
581 cylinders. Slice 1 (0-1 mm: black), slice 2 (1-2 mm: red), slice 3 (2-3 mm: blue), slice 4 (3-4 mm:
582 purple) and slice 5 (4-5mm: green). 5 mm height agar cylinders were cut in five 1 mm width slices to
583 monitor lysozyme concentration as a function of distance to gelatin-based films with lysozyme at
584 regular time intervals.

585 **Figure 3:** FTIR spectra of gelatin films at wavenumbers of 3700 - 2700 cm^{-1} (A) and 1800 - 800 cm^{-1}
586 (B). Non-crosslinked gelatin film without lysozyme (blue curve), crosslinked gelatin film without
587 lysozyme (black curve), crosslinked gelatin film with lysozyme (red curve), and crosslinked gelatin
588 film with lysozyme after release (green curve).

Figure 1

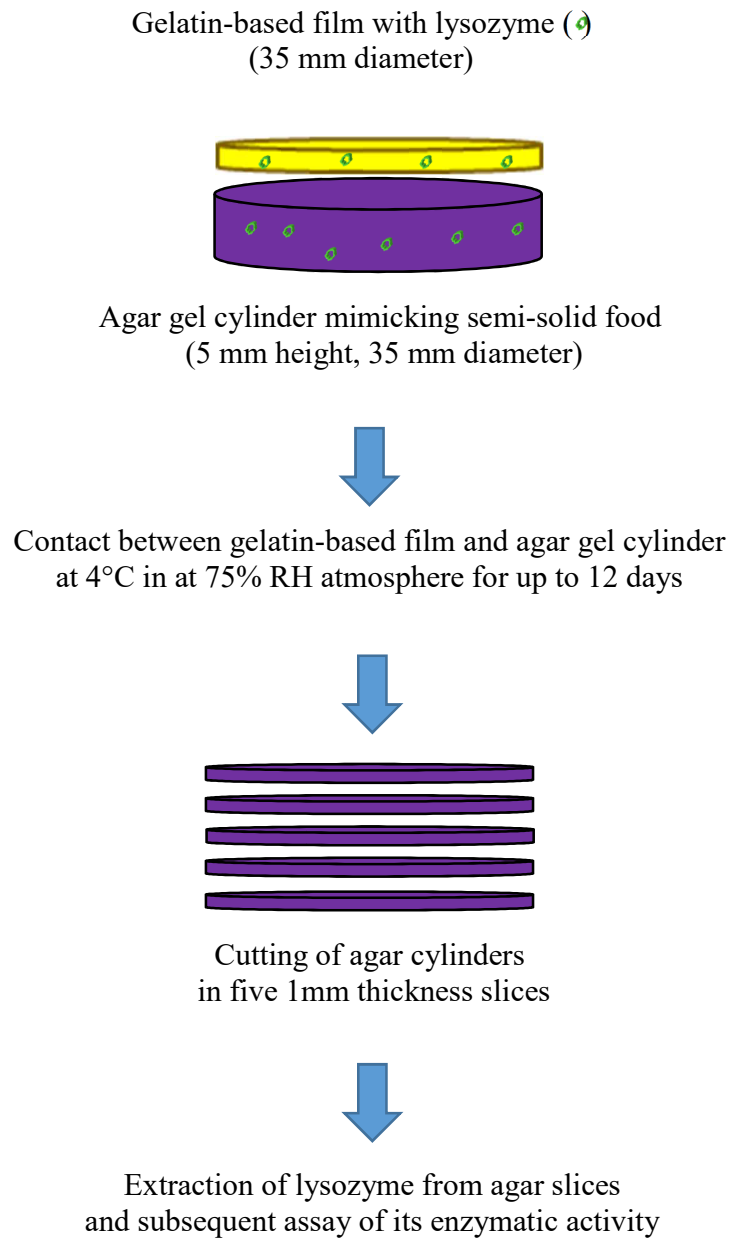
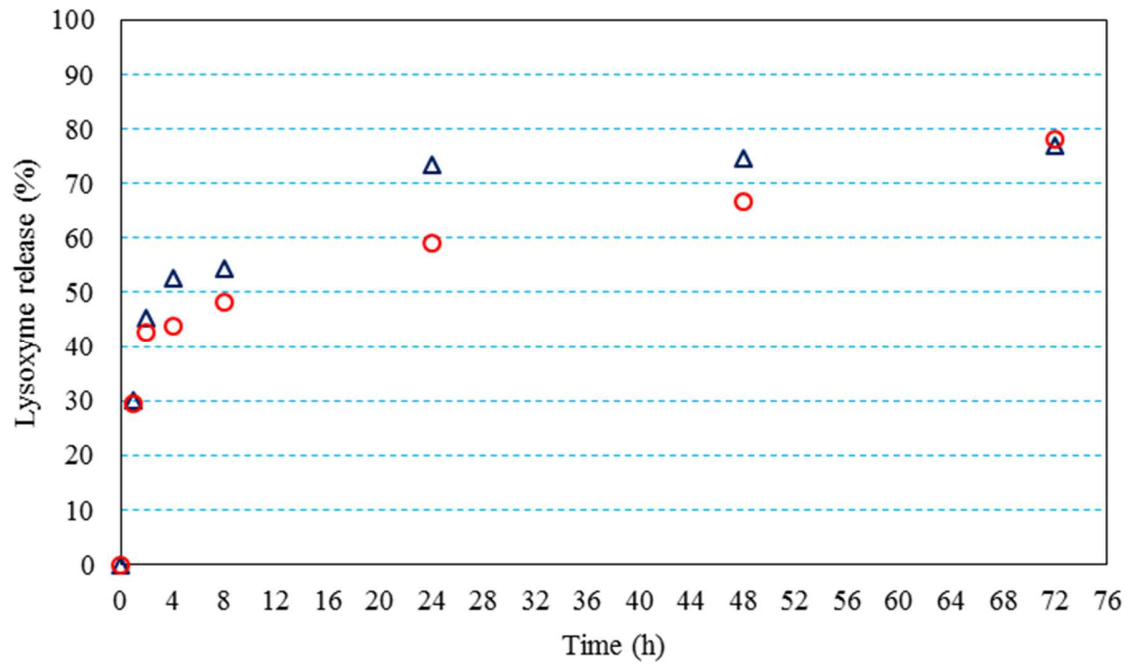


Figure 2

A



B

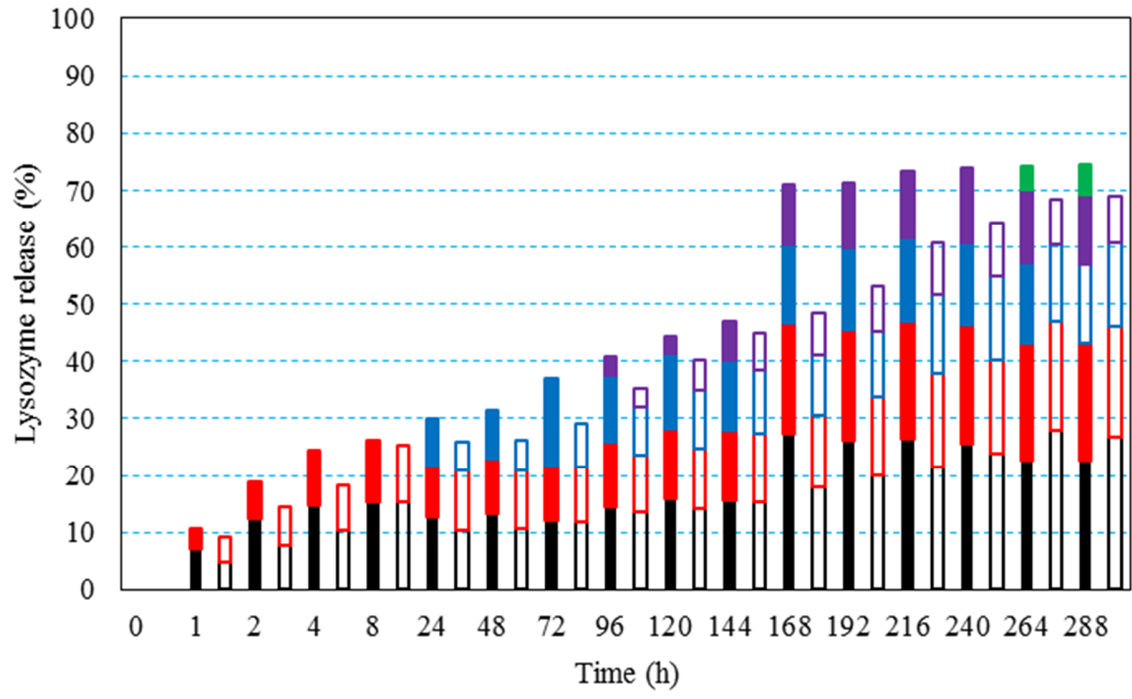
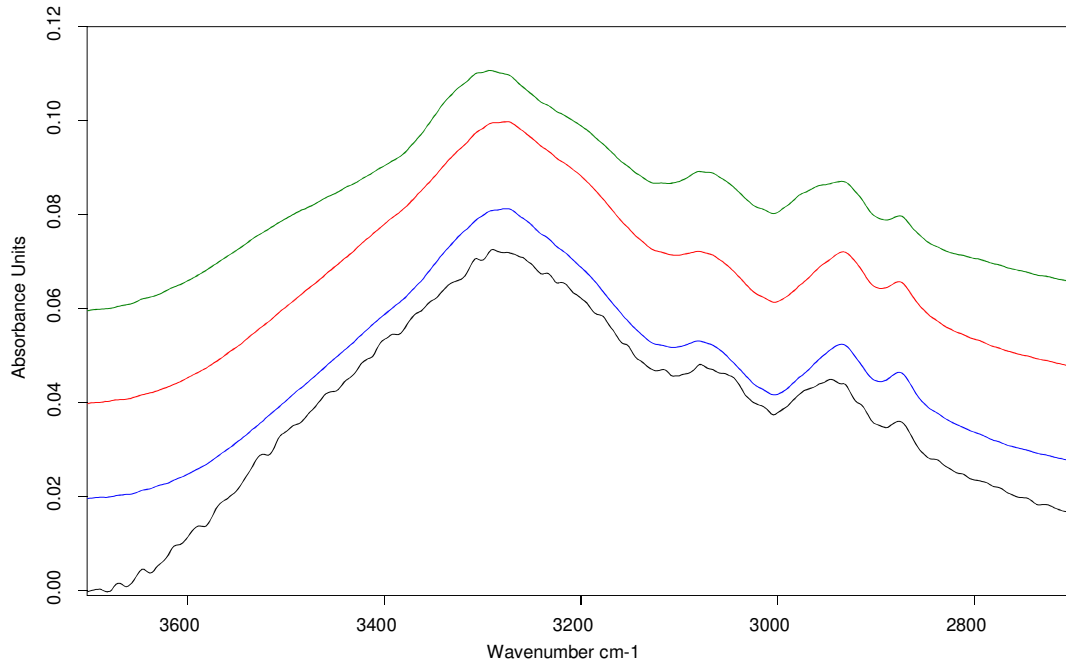


Figure 3

A



B

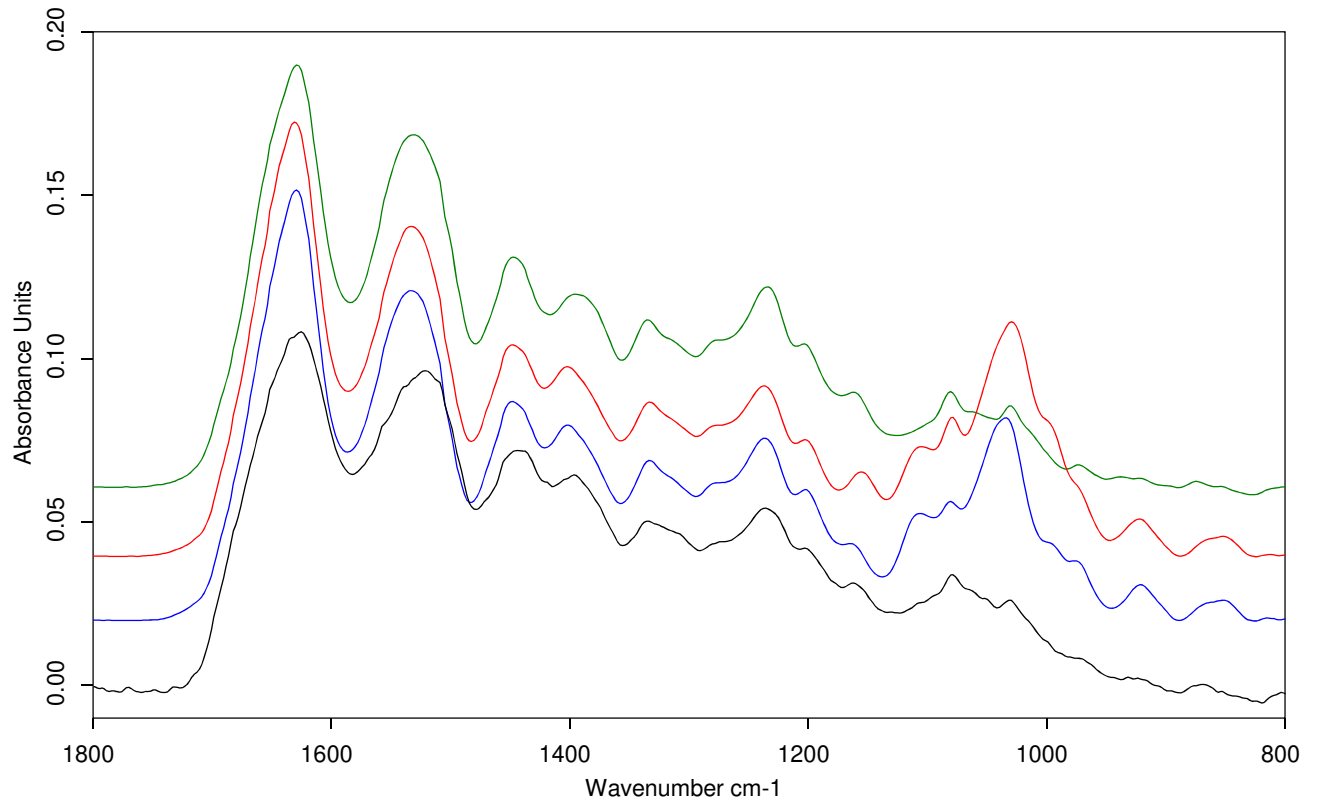


Table 1: Physico-chemical properties of gelatin-based films as a function of MTGase content in the film-forming suspensions (FFS).

MTGase content (g.100mL ⁻¹ FFS)	Thickness (μ m)	Cross-linking degree (%)	Moisture content (%)	Solubility in water (%)	Swelling index (%)	Water vapor permeability ($\times 10^{-9}$ g m ⁻¹ s ⁻¹ Pa ⁻¹)	Tensile strength (MPa)	Elongation at break (%)
Control	253 \pm 20 ^a	0.0 \pm 0.0 ^a	11.3 \pm 0.9 ^a	73.1 \pm 4.7 ^a	84.2 \pm 4.9 ^a	4.6 \pm 0.3 ^a	35.2 \pm 2.0 ^a	67.0 \pm 2.2 ^a
0.14	226 \pm 5 ^{ab}	26.4 \pm 7.4 ^b	10.9 \pm 0.5 ^a	27.3 \pm 2.1 ^b	78.3 \pm 1.3 ^b	4.2 \pm 0.1 ^{ab}	43.5 \pm 1.6 ^b	65.5 \pm 1.3 ^a
0.28	210 \pm 0 ^b	47.0 \pm 2.6 ^c	10.3 \pm 1.4 ^a	29.8 \pm 1.7 ^b	75.6 \pm 0.2 ^{bc}	3.8 \pm 0.1 ^b	45.0 \pm 1.7 ^b	98.6 \pm 29.9 ^b
0.42	173 \pm 28 ^c	52.1 \pm 1.2 ^c	9.6 \pm 0.8 ^a	25.3 \pm 2.3 ^b	72.8 \pm 1.8 ^c	3.2 \pm 0.5 ^c	54.9 \pm 1.3 ^c	84.4 \pm 7.6 ^b

The data represent the mean \pm one standard deviation (n=3). Means with the same letters are not significantly different ($P \leq 0.05$).

Table 2: Estimated parameters of different models for lysozyme release kinetics from control and crosslinked gelatin films to food-mimicking media (stirred buffer (b) or agar gel (g)).

Parameters	k or k_1		k_2 or n		SSE	R^2		RMSE		R^2 /RMSE		
MTGase (g.100mL ⁻¹)	0	0.42	0	0.42	0	0.42	0	0.42	0	0.42	0	0.42
Higuchi (b)	k=0.15	k=0.13	-	-	0.54	0.35	0.32	0.48	0.27	0.22	1.16	2.02
Higuchi (g)	k=0.063	k=0.058	-	-	0.17	0.11	0.89	0.92	0.1	0.08	8.48	11.00
Rigter-Peppas (b)	k=0.49	x	n=0.17	x	0.02	x	0.96	x	0.06	x	15.11	x
Rigter-Peppas (g)	k=0.11	k=0.09	n=0.37	n=0.4	0.14	0.09	0.92	0.93	0.09	0.07	9.52	11.77
Kopcha (b)	$k_1=0.35$	$k_1=0.28$	$k_2=-0.02$	$k_2=-0.02$	0.06	0.09	0.92	0.86	0.10	0.12	9.22	6.93
Kopcha (g)	$k_1=0.07$	$k_1=0.06$	$k_2=0$	$k_2=0$	0.11	0.17	0.90	0.92	0.08	0.1	8.48	10.68

-: not relevant, x: absence of fitting, SSE: Sum of Squared estimate of Errors, R^2 : coefficient of determination, RMSE: Root Mean Square Error

Table 3: Main absorption bands of FTIR spectra (with corresponding maximum absorption wavenumbers (in cm^{-1}) and corresponding attribution of gelatin films components.

MTGase (FTIR spectrum not shown)	Lysozyme (FTIR spectrum not shown)	Control non crosslinked gelatin film (without lysozyme)	non crosslinked gelatin film	Crosslinked gelatin film (without lysozyme)	Crosslinked gelatin film with lysozyme	Crosslinked gelatin film after lysozyme release	Description	References
	3270 cm^{-1}	3281 cm^{-1}		3283 cm^{-1}	3278 cm^{-1}	3295 cm^{-1}	- amide A: N-H stretching coupled with hydrogen bonding	Nagarajan et al., 2012; Liu et al., 2017 ; Barth, 2007
		3077 cm^{-1}		3070 cm^{-1}	3079 cm^{-1}	3075 cm^{-1}	- amide B: asymmetric stretching of C-H and NH_3	Nagarajan et al., 2012
	2934 cm^{-1}	2936 cm^{-1}		2944 cm^{-1}	2933 cm^{-1}	2936 cm^{-1}	- C-H stretching vibrations of $-\text{CH}_2$ (asymmetric)	Nandiyanto et al., 2019
2916 cm^{-1}							- C-H stretching vibrations of $-\text{CH}_2$ (asymmetric)	Nandiyanto et al., 2019
	2873 cm^{-1}	2875 cm^{-1}		2875 cm^{-1}	2878 cm^{-1}	2878 cm^{-1}	- C-H stretching vibrations of $-\text{CH}_2$ (symmetric)	Nandiyanto et al., 2019
1637 cm^{-1}	1639 cm^{-1}						- amide I: mainly C=O stretching ; C-N stretching vibrations	Liu et al., 2017; Barth, 2007
		1629 cm^{-1}		1627 cm^{-1}	1631 cm^{-1}	1629 cm^{-1}	- hydrogen bonding in combination with COO	Nagarajan et al., 2012
		1534 cm^{-1}		1523 cm^{-1}	1534 cm^{-1}	1532 cm^{-1}	- amide II: mainly N-H and C-N stretching vibrations	Liu et al., 2017; Barth, 2007
	1233 cm^{-1}	1238 cm^{-1}		1236 cm^{-1}	1237 cm^{-1}	1236 cm^{-1}	- amide III: vibrations in C-N (stretching) and N-H groups of bound amine (deformation) - amino acids signature: vibrations of CH_2 groups of glycine (backbone) and/or proline side chains	Wang et al., 2015 ; Nagarajan et al. 2012
1077 cm^{-1}		1081 cm^{-1}		1080 cm^{-1}	1080 cm^{-1}	1081 cm^{-1}	- C-O stretching vibrations of short peptide chains	Nagarajan et al., 2012
		1036 cm^{-1}		1034 cm^{-1}	1032 cm^{-1}	1031 cm^{-1}	- interaction between glycerol (C-O stretching) and gelatin - C-O stretching vibrations of short peptide chains	Nagarajan et al., 2012